# Studies on the Power Requirement of Mixing Impellers (IV) : Empirical Equations Applicable for a Wide Range

AUTHOR(S):

NAGATA, Shinji; YAMAMOTO, Kazuo; YOKOYAMA, Tōhei; SHIGA, Shūjiro

# Studies on the Power Requirement of Mixing Impellers (IV)

—Empirical Equations Applicable for a Wide Range—

By

Shinji NAGATA, Kazuo YAMAMOTO, Tōhei YOKOYAMA
and Shūjiro SHIGA

(Received May 6, 1957)

**Abstract**

The present authors have already reported on the empirical equations for the power requirement of paddle agitators.[1] In this report, equations for the three ranges of high, medium, and low viscosity were made and equations for the maximum power required under fully baffled conditions were also formed separately.

Although the results are accurate, these equations are not always convenient because of the complexity in deciding which form to be used.

On the basis of a reasonable assumption derived from the essential concept of power consumption, the authors derived an empirical equation which covers wide ranges of power data as follows:

$$N_P = \frac{A}{R_e} + B\left(\frac{10^3+1.2R_e^{0.66}}{10^3+3.2R_e^{0.66}}\right)^p \left(\frac{H}{D}\right)^{(0.35+b/D)} (\sin\theta)^{1.2} \tag{27}$$

where

$$A = 14+(b/D)\{670(d/D-0.6)^2+185\} \tag{19}$$

$$B = 10^{\{1.3-4(b/D-0.5)^2-1.14(d/D)\}} \tag{22}$$

$$p = 1.1+4(b/D)-2.5(d/D-0.5)^2-7(b/D)^4 \tag{23}$$

The maximum power consumption of paddle agitators can also be calculated by Eq. (27) by substituting $Re$ with the values of $R_c$ and $R_\theta$ which can be obtained by the following equations:

For the paddle having a blade angle of 90°,

$$R_c = \frac{25}{(b/D)}(d/D-0.4)^2 + \left\{\frac{b/D}{0.11(b/D)-0.0048}\right\} \tag{28}$$

For the paddle having an arbitrary angle of $\theta$,

$$R_\theta = 10^{4(1-\sin\theta)}R_c \tag{30}$$

Fairly good agreements were obtained between those values calculated by the equations and those obtained by the experiments.

## 1. Basic concept for the derivation of empirical equations.

The authors have reported the relation between the flow pattern in the agitation vessel and the power consumption. The outline of the results is as follows.

Two kinds of vortices are recognized in an agitation vessel, i.e., the cylindrical rotating zone which rotates with the same speed as that of blades in the central part of a vessel, and the free vortex zone which rotates outside of it. The schematic diagram is shown in Fig. 1a. The central area of the paddle *a b c d* can be assumed to have no relation to the power consumption. On the contrary, the outer part of the paddle *A a d D* and *B b c C* will have an important bearing upon the power consumption. The higher the liquid viscosity, the smaller the cylindrical rotating zone will be. When Reynolds number approaches the critical value between laminar and turbulent flows, the radius of the cylindrical rotating zone ($r_c$) becomes very small in size and the whole paddle area begins to influence the power consumption. As the result, the power consumption reaches a maximum value which can probably be assumed to be equal to the maximum power under fully baffled conditions. Without question there exist other sorts of vortices such as $V_1V_1'$ and $V_2V_2'$ even in the range of low viscosity; however, it is considered that they have relatively less bearing upon the liquid flow. The higher the liquid viscosity, the weaker the vortex motion around the agitator axis and, at the same time, the region of secondary circulating flow is confined only about the axis, blades and vessel walls as shown in Fig. 1(b), and the effect of friction due to viscosity becomes the controlling factor of the power consumption.

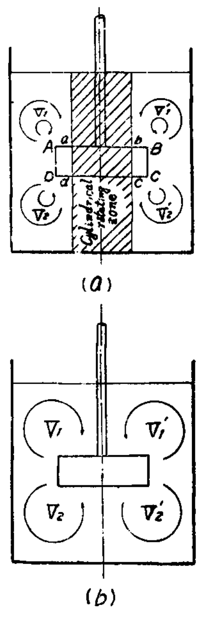


Fig. 1. Schematic diagam showing two sorts of vortices in an agitated vessel.

According to these considerations the power consumption in the range of perfectly tubulent flow and that in the range of perfectly laminar flow will have to be discussed separately. The flow in an agitation vessel, however, has no distinct critical Reynolds number such as in the case of a pipe line flow and the laminar flow changes gradually to turbulent. Thus the power consumption in the transitional range, will rationally be expressed by the equation in which both influences are taken into consideration.

First of all, let the case be considered where turbulent flow predominates.

Fig. 2 shows the schematic diagram of tangential velocity distribution of fluid in an agitation vessel. In this figure, the tangential velocity of blades is shown by $\overline{OAA'}$ while that of liquid, by $\overline{OAA''}$. Therefore, the relative velocity ($u_r$) is equal to $(AA'-AA'')$.

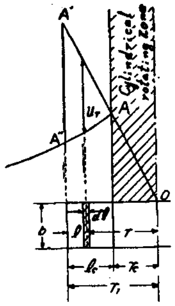

Fig 2. Diagram showing the relative velocity distribution between paddle and liquid.

Now, considering the element of blade $dl$, the force of resistance by liquid, $dF$, can be written as follows.

$$dF = K\rho u_r^2 bdl \qquad (1)$$

When $AA''$ is approximately expressed by a straight line, the relative velocity would be assumed to be linear as follows.

$$u_r = cn(l_c - l) \qquad (2)^*$$

Hence, the power consumption in this element, $dP$, becomes:

$$dP = \omega dM = 2n\pi 2rdF = 4n\pi rdF \qquad (3)$$

Using the relation of Eq. (1) and (2), $dP$ becomes,

$$dP = 4\pi bc^2 K\rho n^3 (l_c - l)^2 (r_1 - l)dl \qquad (4)$$

Integratiug the equation between $l=0$ and $l=l_c$, the power acting on the whole blade is obtained.

$$P = 4\pi bc^2 K\rho n^3 \int_0^{l_c} (l_c - l)^2 (r_1 - l)dl = 1/3\pi bc^2 K\rho n^3 l_c^3 (4r_1 - l_c) \qquad (5)$$

As shown by Eq. (5), the size of $l_c$ has an important bearing on the power consumption, but it is very difficult to know the exact values of $l_c$. In this report, let the approximate equation reported in the previous paper[2] be applied.

$$(r_c/r_1) = Re/(10^3 + 1.6Re) \qquad (6)$$

$$r_c = r_1 - l_c \qquad (7)$$

$$\therefore \quad l_c = \left(\frac{10^3 + 0.6Re}{10^3 + 1.6Re}\right)\left(\frac{d}{2}\right) \qquad (8)$$

Substituting Eq. (8) into Eq. (5)

$$P = \frac{\pi c^2 Kbd^4 \rho n^3}{16} \frac{(10^3 + 1.93Re)(10^3 + 0.6Re)^3}{(10^3 + 1.6Re)^4}$$

$$\doteqdot \frac{\pi c^2 Kb}{16}\left(\frac{10^3 + 0.6Re}{10^3 + 1.6Re}\right)^3 \rho n^3 d^4$$

* It would be more reasonable to use the following relations;

$$u_r = 2n\pi(r_1 - r_c^2/r_1)(l_c - l)/l_c \quad \text{or} \quad u_r = 2n\pi(r - r_c^2/r)$$

But a simple equation, such as Eq. (9) is desirous to derive a convenient empirical equation and, for that reason, the relation of the form of Eq. (2) is applied.

$$\therefore \quad \frac{P\cdot g_c}{\rho n^3 d^5} \doteqdot \frac{\pi c^2 K g_c}{16}\left(\frac{b}{d}\right)\left(\frac{10^3+0.6\,Re}{10^3+1.6\,Re}\right)^3 = B'\left(\frac{10^3+0.6\,Re}{10^3+1.6\,Re}\right)^3 \tag{9}$$

Many assumptions have been made to derive Eq. (9). For example, it has been assumed that the liquid in the cylindrical rotating zone had exactly the same angular velocity with that of the impeller-blades, that coefficient $K$ and $c$ in Eq. (1) and (2) were constants, and that the change of $l_c$ corresponding to the change of Reynolds number could be expressed by Eq. (8).

Consequently, it will be more rational if the power equation is assumed as follows and the coefficients and exponents are determined by using the observed values.

$$\frac{Pg_c}{\rho n^3 d^5} = N_P = B\left(\frac{10^3+0.6fRe^{\alpha}}{10^3+1.6fRe^{\alpha}}\right)^p \tag{10}$$

Next, for the range of laminar flow, the power consumption increases proportionally with the liquid viscosity, so that the following equation is available:

$$\frac{P\cdot g_c}{\rho n^3 d^5} = A\left(\frac{d^2 n\rho}{\mu}\right)^{-1} = \frac{A}{Re} \tag{11}$$

Based upon these considerations, the authors suggested the following type of empirical equation as the one which could be applied for both ranges, i.e., laminar and turbulent flow ranges, and carried out the experiments to obtain coefficients and exponents for the equation.

$$N_P = \frac{A}{Re} + B\left(\frac{10^3+0.6fRe^{\alpha}}{10^3+1.6fRe^{\alpha}}\right)^p \tag{12}$$

Generally, the results of the experiments of the power requirement becomes as shown by a solid line in Fig. 3, i.e., the power number ($N_P$) decreases with the increase in Reynolds number ($Re$), but the rate of decrease falls gradually until finally a constant value is reached. The second term of the right hand side in Eq. (12) satisfies the conditions of $B > B[(10^3+0.6fRe^{\alpha})/(10^3+1.6fRe^{\alpha})]^p > B(0.6/1.6)^p$, and shows good agreements with the results of the experiments.

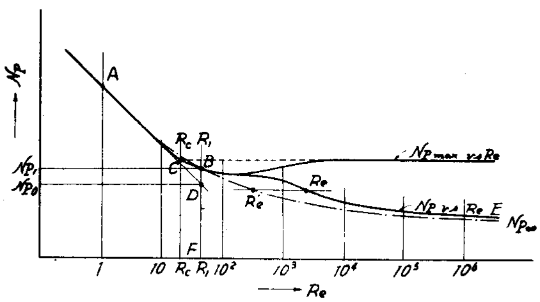


Fig. 3. Schematic diagram showing the method of determination of empirical formula.

On the other hand, when $Re$ becomes smaller than the critical Reynolds number ($R_c$), the first term of the right hand side of Eq. (12) becomes a controlling factor, which is characteristic of laminar flow range.

## 2. Determination of the coefficients in the empirical equation.

**2. 1.** The procedures to determine the coefficients $A$ and $B$.

Fig. 3 is the schematic diagram showing the relation between the power number and Reynolds number for paddles. In this figure, $R_1$ is the boundary Reynolds number between high and medium viscosity ranges as reported before[1], and can be considered as the critical point between the laminar and turbulent flow ranges. These values exist somewhere in the region of $Re$ between 10 and $10^2$. Therefore, the cylindical rotating zone disappears in this vicinity as shown by Eq. (6), and the second term in the right hand side of Eq. (12) takes the value of $B\times 1^p=B$. Noting the power number at $R_1$ as $N_{P_1}$, the following equation is obtained (point $B$ in the diagram).

$$N_{P_1}=\frac{A}{R_1}+B \tag{13}$$

The first term in the right hand side of Eq. (13) is the power number ($N_{P_0}$) at the point of intersection $D$ where the vertical line at $Re=R_1$ comes across with the extended line of $AC$ as shown in Fig. 3. Thus, the following relation is obtained.

$$A=N_{P_0}\times R_1 \tag{14}$$

$$B=N_{P_1}-N_{P_0}=N_{P_1}-A/R_1 \tag{13'}$$

Of course, the value of $A$ can also be calculated by using the power number at another point in the range of perfectly laminar flow; for example, the $N_P$ value at $Re=1$, $(N_P)_{Re=1}$ is equal to $A$.

$$A=(N_P)_{Re=1} \tag{15}$$

**2. 2.** The procedure to determine the exponent $p$.

Let the case be considered where $Re$ becomes an infinity. Under these conditions, $N_P$ gradually approaches to a constant value, which value is presumed by the plots of $N_P$ versus $Re$, and is denoted as $N_{P\infty}$.

$$N_{P\infty}=\lim_{Re\to\infty}\left\{\frac{A}{Re}+B\left(\frac{10^3+0.6fRe^\alpha}{10^3+1.6fRe^\alpha}\right)^p\right\}=B\left(\frac{0.6}{1.6}\right)^p$$

$$p=\frac{\log(B/N_{P\infty})}{\log(1.6/0.6)}=2.35\log\left(\frac{B}{N_{P\infty}}\right) \tag{16}$$

**2. 3.** The procedure to decide $f$ and $\alpha$.

For the sake of convenience, the method of deciding these two factors will be explained in the section **6.**

## 3. Equation to calculate the coefficient $A$.

The values of $N_P$ at $Re=1$, taken from the experimental lines in Fig. 10 and

Fig. 11, are summarized in Table 1. As the result of several trials, it was found that the values of $A$ could be correlated with $(b/D)$ and $(d/D)$ using the from of $14+F(b/D, d/D)$. That is, plotting $(A-14)$ as ordinate against $(b/D)$ as abscissa on a log-log paper, Fig. 4 is obtained. As shown by the figure, all plots, though classified by $(d/D)$ ratio, are approximated by straight lines having slope of 1. Accordingly, $A$ is expressed as follows.

Table 1. Observed values of $A$.

| $b/D$ \ $d/D$ | 0.2 | 0.3 | 0.4 | 0.5 | 0.7 | 0.8 | 0.9 |
|---|---|---|---|---|---|---|---|
| 0.05 | — | 26.3 | — | 22.3 | — | 24.0 | — |
| 0.1 | — | 41.8 | — | 32.5 | 36.2 | 33.6 | 32.7 |
| 0.2 | — | 63.3 | 54.6 | 51.7 | 50.0 | 52.0 | 59.0 |
| 0.3 | — | 84.4 | — | 75.0 | 73.0 | 74.0 | 82 |
| 0.4 | — | — | — | 93.0 | 88.0 | 96.0 | 110 |
| 0.5 | 200 | 135 | 122 | 107 | 110.0 | 122 | 134 |
| 0.6 | — | — | — | — | — | — | 160 |
| 0.7 | — | 190 | 172 | 145 | 146 | 163 | 183 |
| 0.8 | — | — | — | — | — | 182 | 213 |
| 0.9 | — | 228 | 228 | 190 | 175 | 212 | 260 |

$$A=14+(b/D)\cdot F_1(d/D) \tag{17}$$

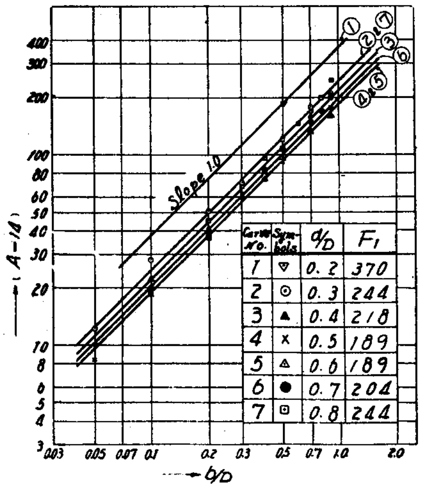


Fig 4. Correlation of $A$ vs. $(b/D)$.

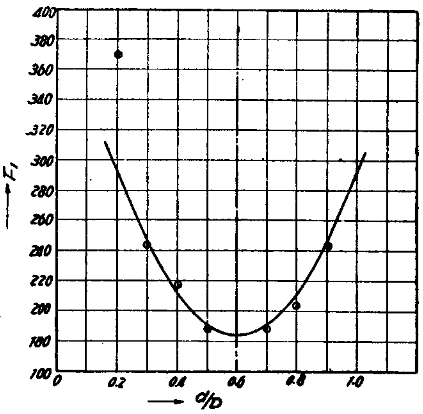


Fig. 5. $F_1$ vs. $(d/D)$.

In this equation, $F_1(d/D)$ is the value of $F$ at $(b/D)=1.0$. Reading off the values of $F_1$ from Fig. 4 and plotting it against $(d/D)$, Fig. 5 is obtained, i.e., an approximately parabolic relationship with the symmetric axis of $(d/D)=0.6$. Then the following relationship is obtained for the range of $(d/D)=0.3\sim0.9$.

$$F_1=670(d/D-0.6)^2+185 \tag{18}$$

Therefore,

$$A=14+(b/D)\{670(d/D-0.6)^2+185\} \tag{19}$$

### 4. Equation for the calculation of *B*.

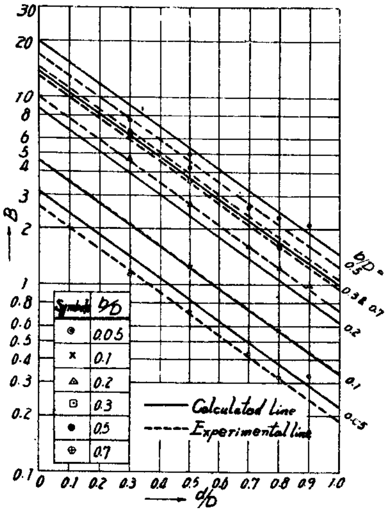


Fig. 6. Correlation of *B* vs. $(d/D)$— Comparison of the observed data (dotted line) and those calc. by Eq (22) (solid line).

Substituting the values of $N_{P1}$ and $N_{P0}$ which are read off from the observed results in Eq. (13′), values of *B* are obtained and plotted against $(d/D)$ in Fig. 6. The parallel line relation is obtained as shown by the broken lines in the diagram, so that the following relation is obtained.

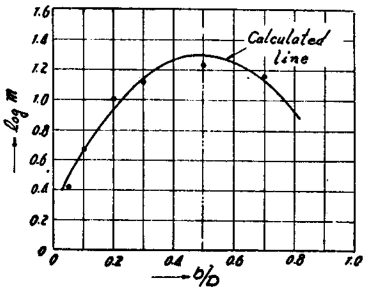


Fig. 7. log *m* vs. $(b/D)$.

$$\log B = \log m - n(d/D) \tag{20}$$

Slope *n* is given as 1.14 by the figure.

The values of $\log m$ in Eq. (20) are equal to the values of $\log B$ at $(d/D)=0$. When the values of $\log m$ are taken from the diagram and plotted against $(b/D)$, Fig. 7 is obtained, giving

$$\log m = -4.0(b/D-0.5)^2+1.3 \tag{21}$$

A curved line in the diagram shows the above equation. Thus, Eq. (20) is determined as follows.

$$B = 10^{\{1.3-4(b/D-0.5)^2-1.14(d/D)\}} \tag{22}$$

The solid line in Fig. 6 shows this equation.

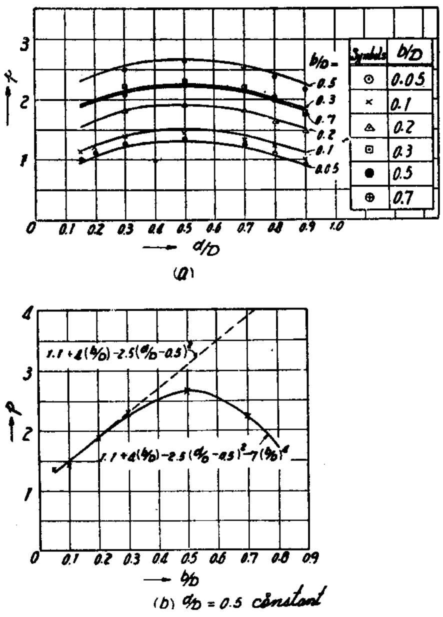


Fig. 8. Correlation of the exponent *p* vs. $(d/D)$ and $(b/D)$.

### 5. Equation to calculate the exponent p.

If the plots of $N_P$ versus *Re* are extrapolated to the larger ranges of *Re*, the values of $N_{P\infty}$ can be presumed. They are shown in Table 2. Substituting the values of $N_{P\infty}$ and $B$ in Eq. (16), the values of $p$ can be obtained, and those values are shown in Fig. 8(a). In Fig. 8 (b), values of $p$ at $(d/D)=0.5$ are plotted against the $(b/D)$ ratio. Thus, the results can be arranged as the following equation.

Table 2. Extrapolated values of $N_{P\infty}$.

| $b/D$ \ $d/D$ | 0.15 | 0.2 | 0.3 | 0.5 | 0.7 | 0.8 | 0.9 |
|---|---|---|---|---|---|---|---|
| 0.05 | 0.8 | 0.62 | 0.42 | 0.23 | 0.15 | 0.13 | 0.12 |
| 0.1 | 1.0 | 0.8 | 0.53 | 0.30 | 0.2 | 0.17 | 0.26 |
| 0.2 | — | — | 0.66 | 0.36 | 0.235 | 0.215 | 0.2 |
| 0.3 | — | — | 0.72 | 0.39 | 0.255 | 0.235 | 0.225 |
| 0.5 | — | — | 0.79 | 0.41 | 0.265 | 0.24 | 0.23 |
| 0.7 | — | — | 0.82 | 0.42 | 0.27 | 0.245 | 0.235 |

$$p=1.1+4(b/D)-2.5(d/D-0.5)^2-7(b/D)^4 \tag{23}$$

## 6. Method to decide the coefficient $f$ and the exponent $\alpha$.

Using the values of $A$, $B$ and $p$ decided above, and putting, at first, $f=1$ and $\alpha=1$ in Eq. (12), the following equation is obtained.

$$N_P=\frac{A}{Re}+B\left(\frac{10^3+0.6\,Re}{10^3+1.6\,Re}\right)^p \tag{24}$$

A chain line in Fig. 3 shows the general form of Eq. (24) and the agreement with observed values is not good in the medium viscosity range. But the chain line must

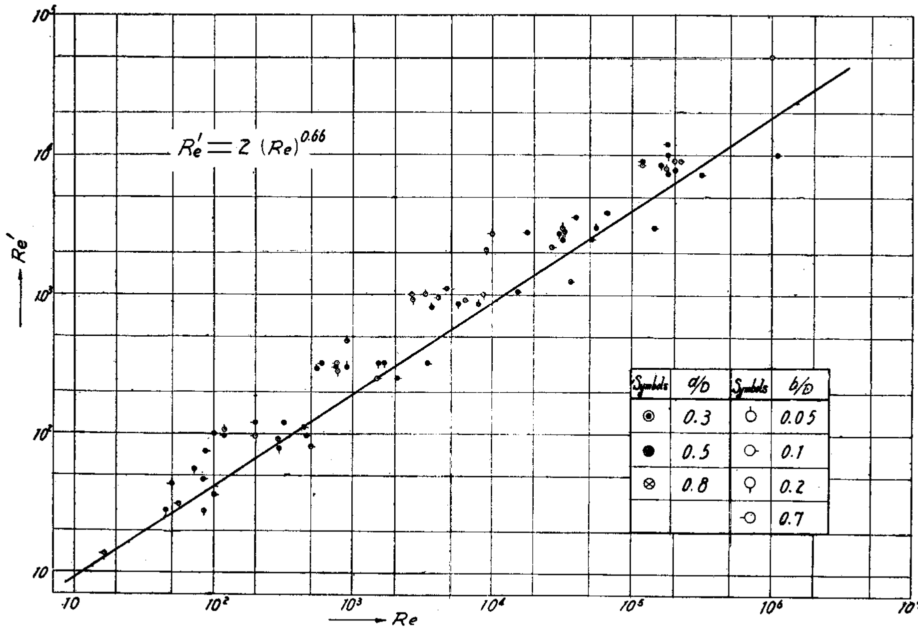


Fig. 9. Correlation of Re′ vs Re.

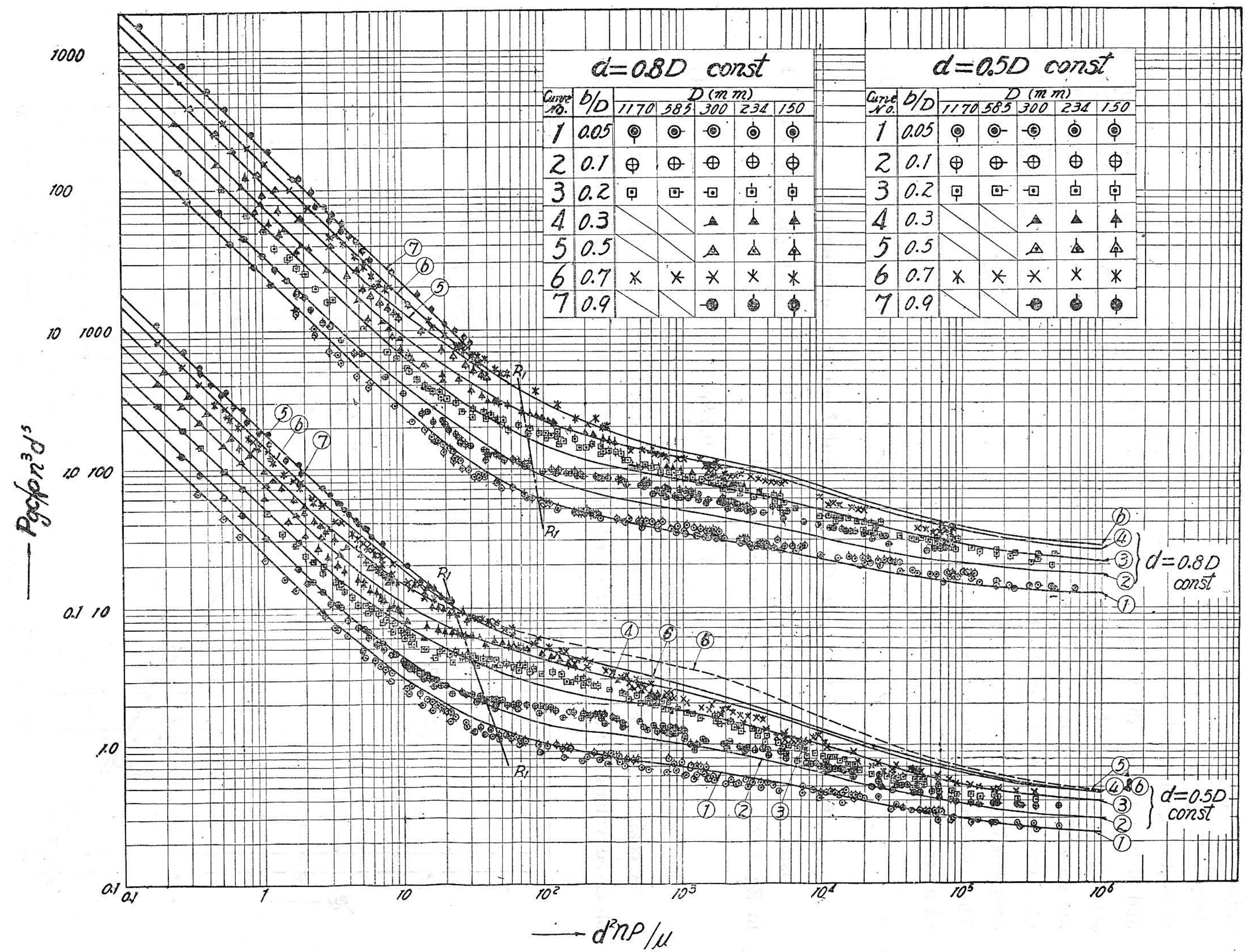


Fig. 10. Relation between power number and Reynolds number for paddles having various width.

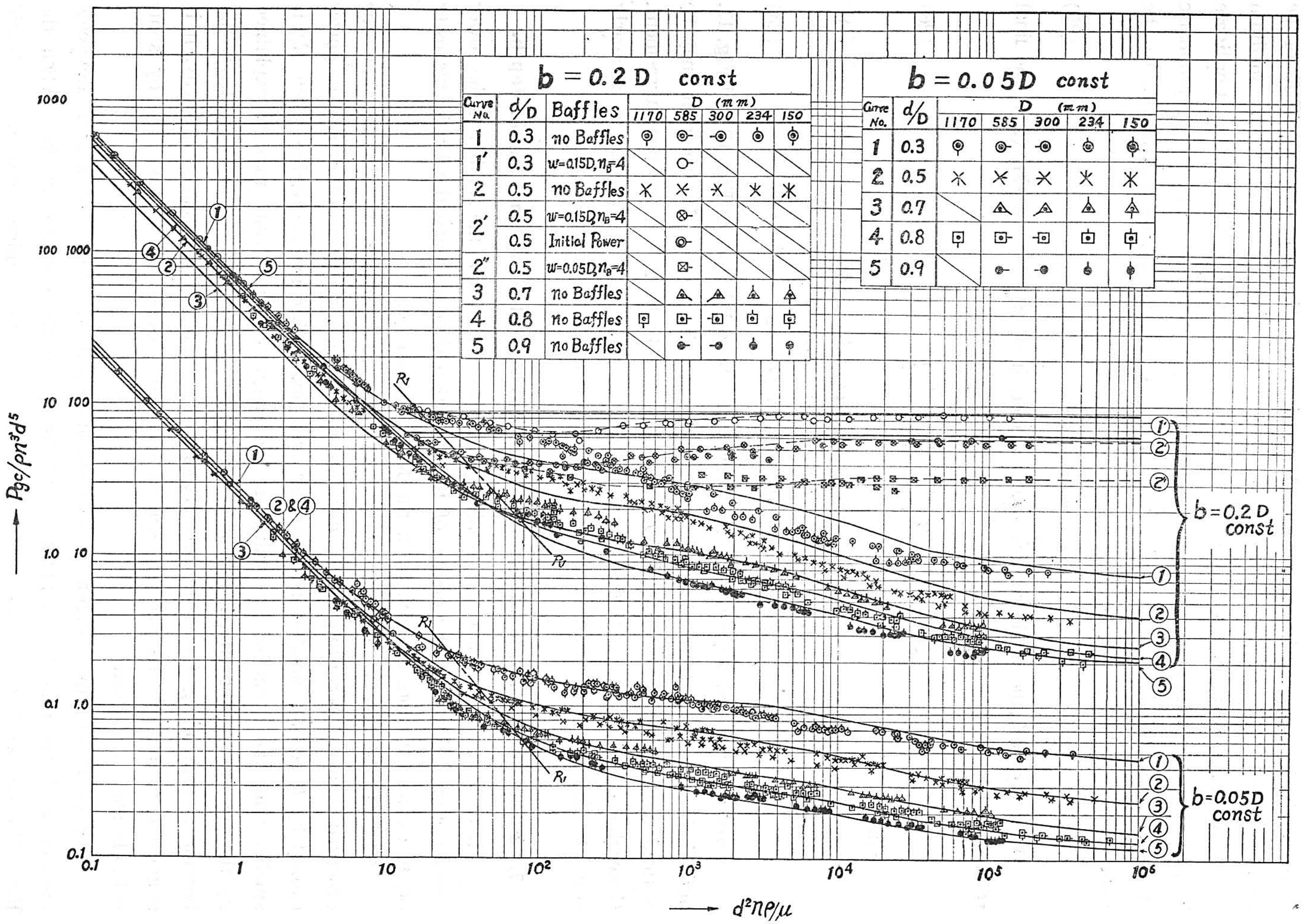


Fig. 11. Relation between power number and Ryenolds number for paddles having various length.

agree with the observed line at three points: *A*, *B* and *E*. Then, reading off *Re* of the observed curve and *Re'* of the calculated line at the same $N_P$ values in the medium viscosity range, and plotting those two values of *Re* and *Re'* as abscissa and ordinate respestively, Fig. 9 is obtained. As can be seen by this figure, there is no systematic deviation with the change in $(d/D)$ and $(b/D)$. Consequently, the relationship can be expressed as follows;

$$Re' = 2Re^{0.66} \tag{25}$$

By using *Re'*, the modified Reynolds number, instead of *Re* in Eq. (24), the final relation is derived as follows.

$$N_P \doteqdot \frac{A}{Re} + B\left(\frac{10^3+1.2Re^{0.66}}{10^3+3.2Re^{0.66}}\right)^p \tag{26}$$

where

$$A = 14+(b/D)\{670(d/D-0.6)^2+185\} \tag{19}$$

$$B = 10^{\{1.3-4(b/D-0.5)^2-1.14(d/D)\}} \tag{22}$$

$$p = 1.1+4(b/D)-2.5(d/D-0.5)^2-7(b/D)^4 \tag{23}$$

Curves calculated by Eq. (26) are shown as the solid lines in Fig. 10 and Fig. 11, and their agreement with the observed values is fairly good. However, it may be noticed that only a dotted line $(d/D=0.5,\ b/D=0.5)$ in Fig. 10 shows poor agreement. Generally speaking, when the width of paddles becomes larger and tend to be nearly equal to the length of paddles, the agreement becomes inferior.

### 7. Effect of the angle of blades to the horizontal plane and liquid depth.

There is no doubt that the smaller the angle of blades, $\theta$, the smaller is the power consumption. However, the degree of the reduction depends upon the liquid viscosity or, to express it more exactly, upon the Reynolds number.

The plotted points along the curves (1), (2), (3) and (4) in Fig. 12 show the observed values. According to the decrease in Reynolds number, differences in power caused by $\theta$ become smaller and samller and finally become negligible when *Re* is smaller than the range of the values in the diagram. This result may be explained by the supposition that the frictional resistance acting upon the surface of blades would become a controlling factor in this region. To express these relations briefly, it is suggested to multiply the second term in the right hand side of Eq. (26) by some suitable correction factor.

The effect of liquid depth is also significant in the range of higher Reynolds number and becomes less significant according to the decrease in *Re*. When the Reynolds number is as low as that corresponding to the laminar flow range, liquid depth has no effect on the power consumption. Hence, it will be convenient to correct

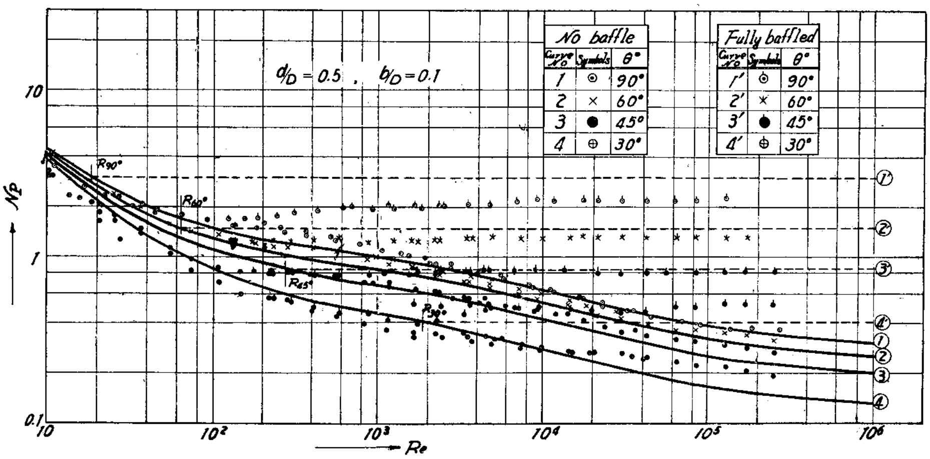


Fig. 12. Effect of blade angles upon the power number at various Re.

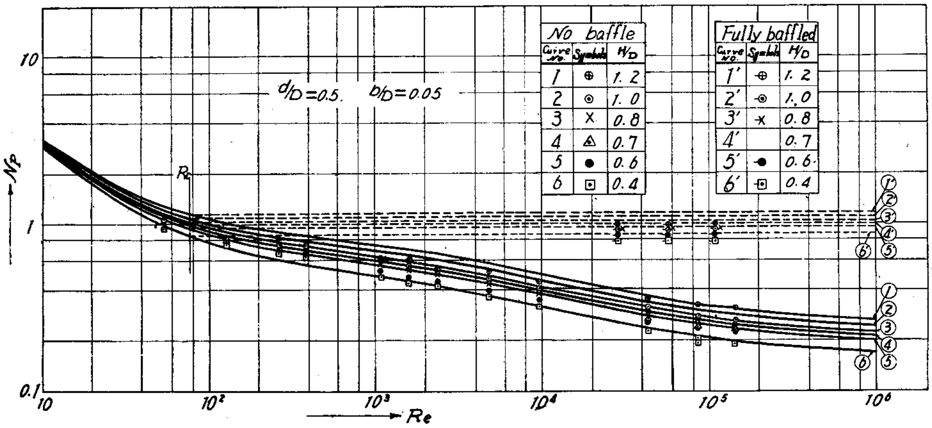


Fig. 13. Effect of liquid depth upon the power number at various Re.

the effect of liquid depth by multiplying the second term of the right hand side of Eq. (26) by a suitable correction factor. From this consideration, the authors obtained the following equation.

$$N_P = \frac{A}{Re} + B\left(\frac{10^3+1.2Re^{0.66}}{10^3+3.2Re^{0.66}}\right)^p \left(\frac{H}{D}\right)^{(0.35+b/D)} (\sin\theta)^{1.2} \tag{27}$$

Curves (1), (2), (3) etc. in Fig. 12 and Fig. 13 show the values of $N_P$ calculated by Eq. (27). These curves coincide well with the observed values. This conclusion has been confirmed by the experiments in the range of $(d/D)=0.3\sim0.8$ and $(b/D)=0.05\sim0.5$, though the diagrams showing those results are omitted.

In fact, the paddles with the impeller diameter smaller than 30 percent of the diameter of agitation vessels, for example $d/D=0.2\sim0.15$, is scarcely used. On the

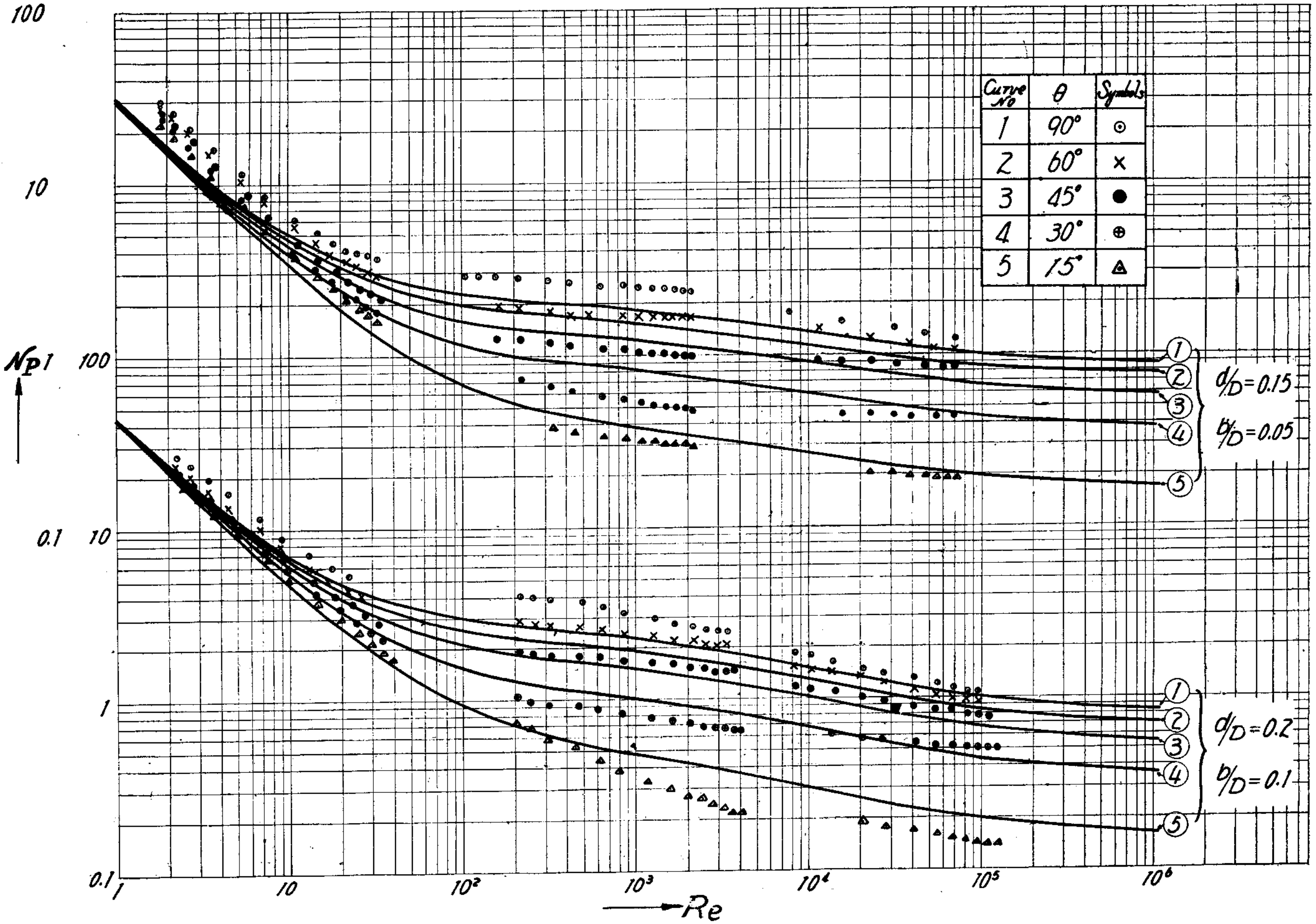


Fig. 14. Relation between power number and Reynolds number for paddles having pitched blades of small diameter.

contrary, the impellers which have inclined blades of the same dimension appear to be frequently used. The authors shall refer to them as simplified propellers.

As mentioned in Fig. 5, the calculated values of $F_1$ deviate largely from the observed values in the range of $d/D < 0.3$, so that the values calculated by Eq. (27) will presumably deviate from those obtained by experiment. However, as shown in Fig. 14, comparatively good agreements are attained. The curves drawn on the diagram are those calculated by Eq. (27).

Consequently Eq. (27) is applicable for the extremely wide ranges that are generally used and shows only slight errors of permissible degree.

The powers consumed by the impellers having various number of blades can be calculated by the approximation method reported[1] previously.

## 8. Maximum power consumption under the fully baffled condstions.

**8.1.** Critical Reynolds number ($R_c$).

As reported in the previous paper,[1] the maximum power is reached where the baffled condition is such that the product $(w/D)$ and $n_B$ is equal to 0.5. It is clear from the discussion in the section **1.** of this paper, that when the viscosity of liquid becomes so high that the cylindrical rotating zone disappears, the power will be equal to the maximum value under the fully baffled conditions. The authors considered the part of this low Reynolds number as the critical Reynolds number between laminar and turbulent flows.

In the mixing system, the transition from laminar to turbulent flow proceeds gradually and the word "critical Reynolds number" is not suitable; but for the present, the Reynolds number where the power is equal to the maximum value is defined as the critical Reynolds number ($R_c$).

The authors used $R_1$ to derive the coefficient $B$ as stated above, presuming $R_1$ as nearly equal to $R_c$. However it is to be noted that the values of $R_c$, here, correspond to the Reynolds number at the points of intersection where the curves of $N_P$ versus $Re$ cross with the curves of $N_{P\max}(=P_{\max}g_c/\rho n^3d^5)$ versus $Re$ which are approximated by horizontal straight lines, as shown in Fig. 3. Arranging the values of $R_c$ for paddles ($\theta=90°$) having various dimension of width and length, the following equation is obtained. The procedure is omitted because it is similar to that used to derive Eq. (23).

$$R_c = \frac{25}{(b/D)}(d/D-0.4)^2+\left(\frac{b/D}{0.11(b/D)-0.0048}\right) \tag{28}$$

**8.2.** Maximum power consumption of paddles having the blade angle of 90°.

As defined in **8.1**, a line of $N_{P\max}$ versus $Re$ comes across with a $N_P$ versus $Re$ line at the Reynolds number of $R_c$ calculated by Eq. (28). Hence, substituting $R_c$

into $Re$ in Eq. (26), $N_{P\max}$ can be calculated. Taking $\sin\theta$ as 1, and substituting $R_c$ into $Re$ in Eq. (27), then the values of $N_{P\max}$ in any liquid depth can be calculated. Further, because $R_c$ is generally a small value, the following simple equation is applicable:

$$N_{P\max} = \frac{A}{R_c} + B\left(\frac{H}{D}\right)^{(0.35+b/D)} \tag{29}$$

The curves (1′) and (2′) in Fig. 11 and (1′) (2′)…(6′) in Fig. 13 are calculated by Eq. (29). These curves on the whole agree well with the observed values. Eq. (29) also shows that the values of $N_{P\max}$ are almost independent of liquid depth.

In Fig. 15, the observed values of $N_{P\max}$ are compared with the calculated values for paddles having various dimensions in width and length, and the agreement is satisfactory.

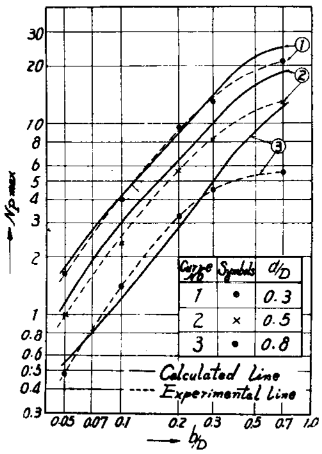


Fig. 15. Comparison of the observed data and the calculated values of $N_{P\max}$.

### 8.3. Maximum power consumption of paddles having inclined blades.

In the case of paddles having inclined blades, the transition from turbulent to laminar flow is so obscure that $R_\theta$ should be defined as $Re$ at the point of intersection where the $N_P$ versus $Re$ curve comes across with the $(N_{P\max})_\theta$ versus $Re$ curve. $R_\theta$ can approximately be calculated from $R_c$ of $\theta=90°$ as follows.

$$R_\theta = 10^{4(1-\sin\theta)} R_c \tag{30}$$

Hence, the maximum power consumption of paddles having inclined blades can easily be calculated by substituting $R_\theta$ into $Re$ in Eq. (27). The curves (1′), (2′), (3′), (4′) in Fig. 12 calculated by this procedure do not necessarily agree well with all of the observed values. However, this is the worst example in agreement and the results of other paddles show better agreement.

## Acknowledgment

The authors wish to express their sincere thanks to H. Maeda, T. Suzue, T. Niki and S. Yoshimura for their cooperation in this study; the experimental data were obtained by them during the past sevral years. Most of the expense of this study was defrayed from the Scientific Research Grant, No. 59354 (1954) and No. 59285 (1956), from the Ministy of Education to which the authors express their hearty appreciation.

**Nomenclature**

| | | |
|---|---|---|
| $A$ | = Proportional constant used in Eq. (11), (12), (26) and (27). | (–) |
| $B$ | = Proportional constant used in Eq. (10), (12), (26) and (27). | (–) |
| $b$ | = Width of impeller blades. | (m) |
| $c$ | = Proportional constant. | (–) |
| $d$ | = Impeller diameter. | (m) |
| $D$ | = Tank diameter. | (m) |
| $F$ | = Force of resistance acting on impeller blades. | (Kg) |
| $f$ | = Correction factor used in Eq. (10). | |
| $g_c$ | = Gravitational conversion factor. | (kg.m/Kg.sec$^2$) |
| $H$ | = Liquid depth. | (m) |
| $K$ | = Proportional constant. | (–) |
| $l$ | = $(r_1-r)$ (refer to Fig. 2) | (m) |
| $l_c$ | = $(r_1-r_c)$ (refer to Fig. 2) | (m) |
| $M$ | = Moment of force acting on the impeller shaft. | (Kg.m) |
| $N_P$ | = $(P\cdot g_c/\rho\, n^3 d^5)$ = Power number | (–) |
| $N_{P\max}$ | = $(P_{\max}\, g_c/\rho\, n^3 d^5)$ = Power number for $P_{\max}$ | (–) |
| $(N_{P\max})_\theta$ | = Power number for $(P_{\max})_\theta$ | (–) |
| $n$ | = Impeller speed in r.p.s. | (1/sec) |
| $n_B$ | = Number of baffle-plates | (–) |
| $P$ | = Power consumption of impellers | (Kg.m/sec) |
| $P_{\max}$ | = Maximum power consumption of impellers | (Kg.m/sec) |
| $p$ | = Exponent used in Eq. (10), (12), (26) and (27). | (–) |
| $r$ | = Radial distance from the axis to any section of impeller | (m) |
| $r_1$ | = Radius of impellers | (m) |
| $r_c$ | = Radius of cylindrical rotating zone | (m) |
| $Re$ | = $(d^2 n\, \rho/\mu)$ = Reynolds number | (–) |
| $Re'$ | = Modified Reynolds number defined as Eq. (25) | (–) |
| $R_1$ | = $Re$ at the transitional points between laminar and turbulent regions. | (–) |
| $R_c$ | = Reynolds number at the point of intersection of $N_{P\max}-Re$ and $N_P-Re$ lines | (–) |
| $R_\theta$ | = Reynolds number at the point of intersection of $(N_{P\max})_\theta-Re$ and $(N_P)_\theta-Re$ lines | (–) |
| $u_r$ | = Relative velocity of impeller and liquid | (m/sec) |
| $w$ | = Width of baffle-plates | (m) |
| $\alpha$ | = Exponent for correction used in Eq. (10) | (–) |
| $\rho$ | = Density of liquid | (kg/m$^3$) |
| $\mu$ | = Viscosity of liquid | (kg/m.sec) |
| $\theta$ | = Angle of blades to the horizontal plane | (–) |
| $\omega$ | = Angular velocity of impeller | (radian/sec) |

### Literature cited

1) S. Nagata, T. Yokoyama and H Maeda: Chem. Eng (Japan) *20*, 582 (1956), Memoirs of the Faculty of Eng. Kyōto Univ. *18*, 13 (1956).
2) S. Nagata, N. Yoshioka and T. Yokoyama: Annual Rep. of Chem. Eng. (Japan), *8*, 43 (1950), Memoirs of the Faculty of Eng. Kyōto Univ. *17*, 175 (1955).